Vibration Analysis of Elastic-Rigid Coupling EMS Maglev System

Shi Xiao-hong，Liu Heng-kun，She Long-hua，Chang Wen-sen
National University of Defense Technology, Changsha, China

Abstract: The vibrant characteristics in the direction of vibration of the multi-DOF maglev system based on the elastic levitation chassis are studied. The elastic levitation chassis is modeled and validated using the finite element method, and the model of the elastic-rigid coupling maglev system is obtained. The design method of the suspending controller is introduced and the relationship between the control parameters and the characteristic frequencies is given. By comparing the calculating results of the elastic-rigid coupling system model, it is proved that the elastic chassis may likely result in the internal resonance of the maglev system.

Keywords: Elastic levitation chassis, internal resonance, maglev, mode analysis

1 Introduction

The dynamic stability of repulsive-force maglev has already been extensively studied in recent years[1]~[3], but the subject of vibration when the system is immovably suspending on the guideway needs more attention. The vibration may happen for various reasons. It is found out in this paper that the levitation chassis, which is designed to be elastic so as to decay the disturbance from the adjacent suspending controllers, impacts the dynamic response of the whole system. The aim of this paper is to explain the leviation chasis's elastic effect on the maglev system by analyzing the dynamic model of the leviation chasis.

2 Model of Elastic-Rigid Coupling System

The maglev is composed of the carriage, the second suspending subsystem, the elastic levitation chassis, the electromagnet, the suspending controller and the guideway[4]. The suspending gap is maintained by the suspending controller through adjusting the current of the electromagnet implemented. Now we give the model of each part.

2.1 Guideway

The guideway is described by the Euler-Bernoulli simple beam and its mode response is

$$w=\sum_{j=1}^{n} q_j \sin\frac{j\pi x_0}{L} \quad \ddot{q}_j=-2\beta\dot{q}_j-\omega_j^2 q_j-\frac{F_e}{2\rho L}\sin\frac{j\pi x_0}{L} \tag{1}$$

where w is the suspending location in the y coordinate, q_j is the j-th generalized coordinate, L is the span, x_0 is the initial position which is corresponding the levitation chassis, β is the equivalent damp, ω_j is the j-th inherent frequency, ρ is the mass per meter, F_e is the electromagnet force, and n is the rank of the mode.

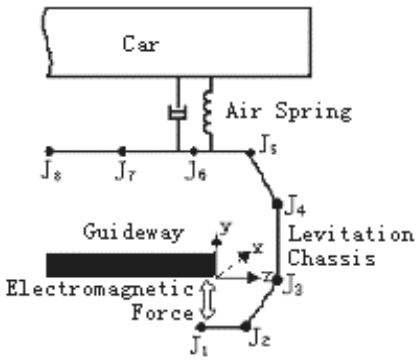

Figure 1. Basic Structure of the Meglev System

Here we assume x_0 = L/2 and n = 1, so the guideway dynamic differential equation is

$$\ddot{w} = -2\beta\dot{w} - \omega_1^2 w - \frac{F_e}{2\rho L} \tag{2}$$

2.2 Suspending controller

The electromagnet force is why the guideway and the levitation chassis is coupled. The coupling is described as:

$$F_e = \frac{\mu_0 N^2 A I^2}{4(y_e - w)^2} \tag{3}$$

where y_e is the displacement of the levitation chassis in the y coordinate, w is the displacement of the guideway, N is the turns of the electromagnet winding, and A is the efficient area of the electromagnet. In practice, the real controlled signal is the voltage instead of the current of the winding. The relationship of the voltage and the current is described as

$$U = RI + \frac{d(LI)}{dt} = RI + \frac{\mu_0 N^2 A}{2(y_e - w)}\dot{I} - \frac{\mu_0 N^2 AI}{2(y_e - w)^2}\left(\dot{y}_e - \dot{w}\right) \tag{4}$$

where U and I are the voltage and current of the electromagnet winding, respectively, and R is the resistance. With (4) we can see that the current lags behind the voltage because of the nonlinear inductance of the the winding. This is one of the main reasons of the instability of the maglev system. In order to make up this delay, we use the cascade method to design the suspending controller[5]. The controller is divided into two part, one is the current loop, the other is the suspending subsystem . The current loop uses current feedback and suspending subsystem uses gap and velocity feedback. A integral control of the gap error is used to hold the given stable gap(viz. y_e=s_0). So the controller model is

$$U_a = k_{c1}\left[U_c - U_f + \int (y_e - w - s_0)dt\right] = k_{c1}\left[U_c - k_{c2}I + \int (y_e - w - s_0)dt\right] = RI + 2k\left(\frac{\dot{I}}{y_e - w}\right) \tag{5}$$

$$U_c = k_d\left(\dot{y}_e - \dot{w}\right) + k_p\left(y_e - w\right) \tag{6}$$

where U_a is the actual winding voltage, U_c is the control voltage that the suspending subsystem outputs, k_{c1} is the current feedback coefficient, k_{c2} is the plus of the current sensor, k_d and k_p are the feedback plus of the velocity and gap, respectively, and s_0 is the given stable gap. Now the problem is to choose the control parameters which should ensure the stability and leads to the satisfying dynamic response.

In the controller design process, the disturbance of the guideway is ignored to reduce the design difficulty. For the same reason, the chassis and upwards parts are regard as an unit one which mass is m. Now from (3) ~ (6) we can deduce that the controller consists of two characteristic generalized modes: one is the current loop frequency ω_m and damping ξ_m, the other is the suspending frequency ω_c and damping ξ_c. The connections between these two mode and control parameters are showed as

$$k_{c1} = -\omega_c^2\omega_m^2\sqrt{\frac{mk}{g}} \qquad k_{c2} = \frac{\sqrt{mg/k}\left[Rs_0 - 4k\left(\xi_c\omega_c + \xi_m\omega_m\right)\right]}{ms_0\omega_c^2\omega_m^2}$$

$$k_p = \frac{8gk\sqrt{mg/k}\left(\xi_c\omega_c + \xi_m\omega_m\right)}{ms_0\omega_c^4\omega_m^4} + \frac{2\left(\xi_c\omega_m + \xi_m\omega_c\right)}{\omega_c\omega_m} \quad k_d = \frac{-\omega_c^2 - 4\xi_c\xi_m\omega_c\omega_m - \omega_m^2}{\omega_c^2\omega_m^2} \tag{7}$$

After choosing the frequency and damping of the current loop and the suspending subsystem, the value of the controller parameters are readily determined. The practice shows that this controller can realize the fast tracing of the current and hold robust when the load changes.

2.3 Elastic levitation chassis

The elastic levitation chassis can be modeled by eight nodes as shown in Fig. 1. Beside the gravity, the first node accepts the electromagnetic force F_e and the sixth accepts the air spring force F_a. So the model is

$$M\ddot{y} + C\dot{y} + K\left(y - y^0\right) = f_{8\times1} = \left[m_8 g \quad m_7 g \quad m_6 g + F_a \quad m_5 g \quad \cdots \quad m_2 g \quad m_1 g - F_e\right]^T \tag{8}$$

where y is a vector describing the displacement of each node in y coordinate, y^0 is the initial node's position, M, C and K are the mass, damping and stiffness matrix, respetively, and the dimension of each matrix is 8×8. The value of the matrix coefficient will be explained in the third part.

2.4 Second suspending subsystem

The relationship of the force and distortion of the air spring can be considered to be linear in the practice. So we can use the following equation to analyze the second suspending subsystem

$$F_a = k_a\left(y_6 - y_a + a\right) + c_a\left(\dot{y}_6 - \dot{y}_a\right) \tag{9}$$

where the constant a is the initial length of the spring, y_a is the displacement of the carriage in y coordinate, k_a is the stiffness of the air spring, C_a is the damping of the second suspending subsystem.

2.5 Carriage

Because of its huge stiffness coefficient, the carriage is regarded as a rigid body:

$$m\ddot{y}_a = mg - k_a\left(y_6 - y_a + a\right) - c_a\left(\dot{y}_6 - \dot{y}_a\right). \tag{10}$$

2.6 Model of the magelv

Choose the state variable as:

$$x = \left[y_a \quad y_8 - y_8^0 \quad \cdots \quad y_1 - y_1^0 \quad w \quad I/(y_1 - w) \quad \dot{y}_a \quad \dot{y}_8 \quad \cdots \quad \dot{y}_1 \quad \dot{w} \quad \left[I/(\dot{y}_1 - w)\right]\right]^T.$$

Using (1)-(10), the dynamic differential equations of the maglev system is:

$$\dot{x}_{1\sim11} = I_{11*11}x_{12\sim22} \quad \dot{x}_{12} = g - \frac{k_a}{m}\left(x_1 - x_4 + a\right) - \frac{c_a}{m}\left(x_{12} - x_{15}\right) \tag{11}$$

$$\left[\dot{x}_{13\sim20}\right] = -M^{-1}K\left[x_{2\sim9}\right] + M^{-1}\begin{bmatrix} m_8 g \\ m_7 g \\ m_6 g + k_a\left(x_1 - x_4 + a\right) + c_a\left(x_{12} - x_{15}\right) \\ m_5 g \\ \vdots \\ m_2 g \\ m_1 g - kx_{11}^2 \end{bmatrix} \tag{12}$$

$$\dot{x}_{21} = -2\beta x_{21} - \omega_1^2 x_{10} - kx_{11}^{\ 2}/\left(2\rho L\right) \tag{13}$$

$$\dot{x}_{22} = \frac{k_{c1}}{2k}\left[x_9 - x_{10} - s_0 + k_p(x_{20} - x_{21}) + k_d\left(2\beta x_{21} + \omega_1^2 x_{10} + \frac{k x_{11}^{\ 2}}{2\rho L} + \sum_{i=1}^{8}\left[(M^{-1}K)x_{1+i} + M_{8,i}^{-1}F_i \right] \right) \right] \qquad (14)$$
$$- \frac{k_{c1}k_{c2} + R}{2k}\left((x_9 - x_{10})x_{22} + (x_{20} - x_{21})x_{11} \right)$$

3 Modeling the elastic levitation chassis

Based on the definition of the mass and stiffness matrix, we model the eight nodes dynamic response model of the elastic chassis with the aid of the finite element analysis method. We will also use the finite element method to prove the matrix validity. In this paper, we consider the levitation chassis structure in the Changsha Middle-low Speed Maglev Laboratory. Because the levitation chassis has a small damp, the damp matrix *C* is ignored.

The finite element method is used to aid the modeling of the matrices *M* and *K* because the chassis structure is complex and the element value calculation is difficult. The modeling process of chassis is [6]: Firstly, use the software, like Pro_e or Solidworks, to construct the 3D structure of the chassis; Secondly, save the structure as .igs format and import it into the finite element analysis software ANSYS. Note that we must carefully find the equivalent area of the corresponding node for during the analysis process the object we dealt with is not nodes but areas. When we calculate the stiffness matrix element in the first row, the equivalent areas except the first one is fixed, so the other seven nodes has no free DOF. Then put 1 millimeter restriction on the first equivalent area, and use this structure analysis function of ANSYS to solve the problem. After the calculation finished, the total counterforce of each area should be read out and multiplied by 1000. These numbers are just the values of the first row element. The other stiffness row element can be calculated in the similar way. When calculating the mass matrix elements, the load added to the area is not the unit displacement but the acceleration.

The matrices *M* and *K* are calculated as listed in Table 1. Because *M* and *K* are symmetric, the table only lists the upper-triangular part of the two matrices. Based on Table 1 and (8), the eigenvalues of the maglev system are

121.658，240.871，321.847，380.012，494.699，664.733，746.782，905.853

Simultaneously, the mode analysis result of ANSYS is：

116.61，242.27，312.58，390.72，540.83，679.97，789.24，943.44

Comparing these two set of results we can see that the error is 2% in the low frequency range and increase up to 5% in the high frequency range. This is due to the limited nodes selection. We only choose 8 nodes, which is equivalent to truncating the high frequency mode of the system. But in the whole frequency range the error is acceptable, so next we will use the data in Table 1 to analyze the vibration characteristics of the maglev.

Table 1 The mass and stiffness matrix value of the elastic levitation chassis

Mass Matrix				Stiffness(1.0e+07)			
Index	Value	Index	Value	Index	Value	Index	Value
(1,1)	24.1071	(5,5)	52.5993	(1,1)	0.6563	(5,5)	-0.6354
(2,2)	48.2437	(5,6)	5.9407	(2,2)	-0.6563	(5,6)	0.9318
(2,3)	6.9795	(6,6)	59.7711	(2,3)	1.2250	(6,6)	-0.2965
(3,3)	44.3865	(6,7)	6.6010	(3,3)	-0.5687	(6,7)	0.5489
(3,4)	10.1250	(7,7)	62.4000	(3,4)	1.3465	(7,7)	-0.2524
(4,4)	43.6022	(7,8)	7.2740	(4,4)	-0.7778	(7,8)	0.4677
(4,5)	9.7793	(8,8)	31.8760	(4,5)	1.4131	(8,8)	-0.2153

4 The vibration analysis of the maglev suspending system

Because of the trivially variable gap, the mode analysis of the diagnostic maglev system (i.e. the linearization system) can indicate the dynamic vibrant response of the real system. In this paper, we use the parameters of the Changsha test runs:

ka = 40000, ca = 400, a = 0.3 m, L = 25, β = 0.01, ρ = 3000 kg/m, ω_1 =90 rad/s, s_0 = 0.01 m, R = 3, k = 0.0035

From (7) we can see that the control parameters are closely related with the load. If the load varied greatly while the parameters of the controller keeps unchanged, the system will become instable. In real runs, the control parameters are always adjusted according to (7) by measuring the current stable value and deriving the load. Here the current loop frequency is 50 Hz and the suspending subsystem frequency is 7 Hz, the damp radios are all 0.7.

The mode analysis result is shown in Table 2 with different load. Because the maglev system has damp, the calculated vibration modes are all complex. Im(λ) is the imaginary part corresponding to the vibration frequency and Re(λ) is the real part corresponding to the vibration attenuation coefficient. The table only lists the low attenuating vibration mode in order to observe the main vibration phenomena of the maglev system. Table 2 shows that the attenuating coefficients change accordingly when the load varies. However, the vibration frequency of each mode keeps unchanged.

Table 2 The vibration frequencies of the maglev in different load

m	Re(λ)	Im(λ)	m	Re(λ)	Im(λ)
3000	-0.0662	3.64511	4000	-0.0496	3.15688
	-0.0463	426.932		-0.0435	426.932
	-0.0435	0.03374		-0.0401	0.02921
	-0.0100	89.9525		-0.0100	89.9525
	-7.99e-5	308.169		-7.99e-5	308.169
	-4.29e-6	277.753		-4.32e-6	277.753
5000	-0.0435	426.932	6000	-0.0435	426.932
	-0.0397	2.82367		-0.0331	2.57769
	-0.0359	0.02612		-0.0327	0.02384
	-0.0100	89.9525		-0.0100	89.9525
	-7.98e-5	308.169		-7.98e-5	308.169
	-4.35e-6	277.753		-4.36e-6	277.753

In this paper, the vibration analysis results of the rigid levitation chassis are also given to compare the dynamic effects of the rigid with elastic chassis. Similarly, only the low attenuating mode (only one) is listed：

m = 3000：Re(λ) ＝ -0.0666332，Im(λ) ＝ 3.65098

m = 4000：Re(λ) ＝ -0.0499778，Im(λ) ＝ 3.16194

m = 5000：Re(λ) ＝ -0.0399836，Im(λ) ＝ 2.82812

m = 6000：Re(λ) ＝ -0.0333205，Im(λ) ＝ 2.58173

Comparing these result with those in Table 2, it is easy to conclude that because of the elastic levitation, several low attenuated modes are added to the linearized maglev system. When the levitation is elastic, some inherent frequencies have common divisors, e.g., 277.753 ≈ 3×89.9525, 531.046 ≈ 277.753×2, etc.

5 Conclusions

Because of the introduction of the elastic levitation chassis, the amount of the vibration frequencies is largely increased and some of them are commonly divided[7]. This problem enhances the chances of the system internal resonance: if a vibration mode of certain subsystem is inspired, the vibration will be continuously transferred between the common modes and finally result in the whole system vibration. This kind of vibration is difficult to adjust by controller or the second appending subsystem, so the elastic levitation chassis must be selected carefully during the system design process.

References

1 Y.Cai, S.S.Chen, D.M.Rote, H.T.Coffey. Vehicle/Guideway Interaction for High Speed Vehicles on a Flexible Guideway. *Journal of Sound and Vibration*, 1994; 175 (5): 625-646.

2 Xiao Jing Zheng, Jian Jun Wu, You-He Zhou. Numerical Analyses on Dynamic Control of Five Degree of Freedom Maglev vehicle Moving on Flexible Guideways. *Journal of Sound and Vibration*, 2000;235 (1): 43-61.

3 Wu Jianjun, Zheng Xiaojing, Zhou Youhe. Dynamic Characteristic Analysis of Maglev Vehicle with Two Degrees of Freedom on Flexible Guideway. *Journal of Vibration Engineering*, 1999, 12: 439-446

4 Wu Xiangming，The Maglev，Shanghai Scientific & Techincal Publishers，2003

5 Li Yungang, Chang Wensen, Cascade Control of an EMS Maglev Vehicle's Levitation Control Sysytem. *ACTA Automatic Sinica*, 1999; 25: 247~250

6 Hong Qingzhang，ANSYS Didactical Examples，China Railway Publishing House，2002

7 Liu Yanzhu，Chen Wen liang，Mechanic of Vibrations，Higher Education Press，1998